Enhanced Photocatalytic Hydrogen Production Efficiency Using Urea-Derived Carbon Nitride in a Continuous Flow Reactor

Samar Batool,[1] Malek Y. S. Ibrahim,[*1] Florian Ehrlich-Sommer,[1] Stephen Nagaraju Myakala,[2] Shaghayegh Naghdi,[2] and Alexey Cherevan[2]

[1]Redeem Solar Technologies GmbH, Stremayrgasse 16 / IV 8010 Graz, Austria.
E-mail: malek.ibrahim@redeemtechnologies.com

[2]TU Wien, Institute of Materials Chemistry, Getreidemarkt 9/BC/02, 1060, Vienna, Austria.

Supplementary Information

Table of Contents

1. Material Characterization

1.1. XRD

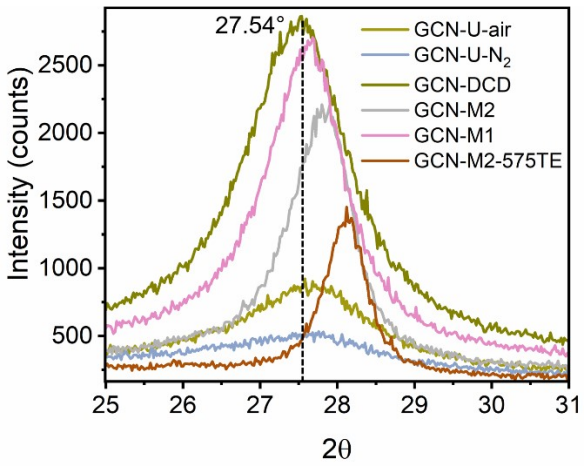

Figure S1 | Powder XRD spectra of GCN-X and GCN-X-TE samples, extended from 25° to 31° showing the shifts in 002 peak.

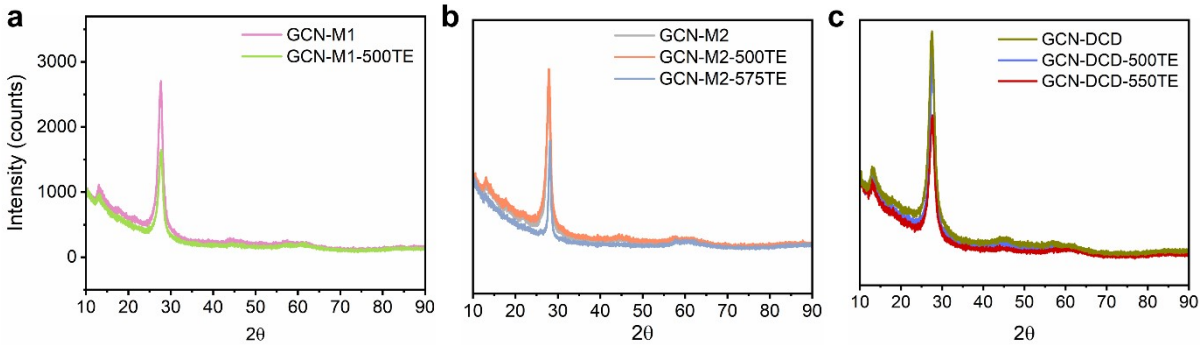

Figure S2 | Powder XRD spectra of GCN-X and GCN-X-TE samples. **a.** GCN-M1 **b.** GCN-M2, and **c.** GCN-DCD.

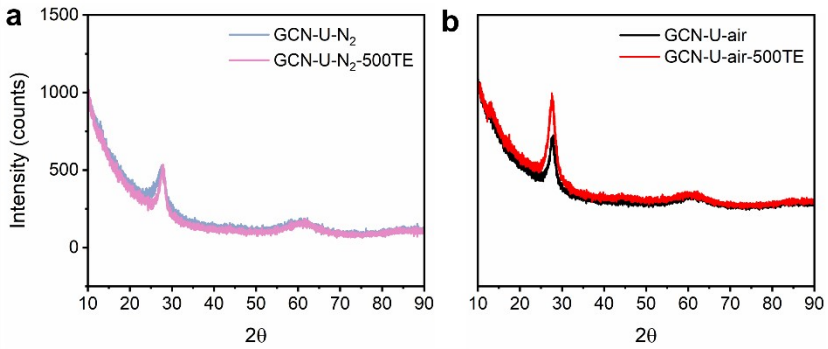

Figure S3 | Powder XRD spectra of GCN-X and GCN-X-TE samples. **a.** GCN-U-N_2, and **c.** GCN-U-air.

1.2. IR

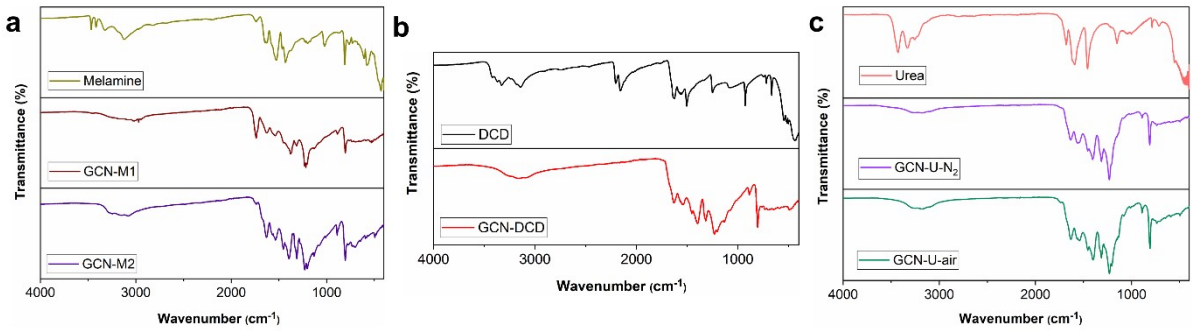

Figure S4 | IR spectra of GCN-X and precursors. **a.** Melamine, **b.** DCD, and **c.** Urea.

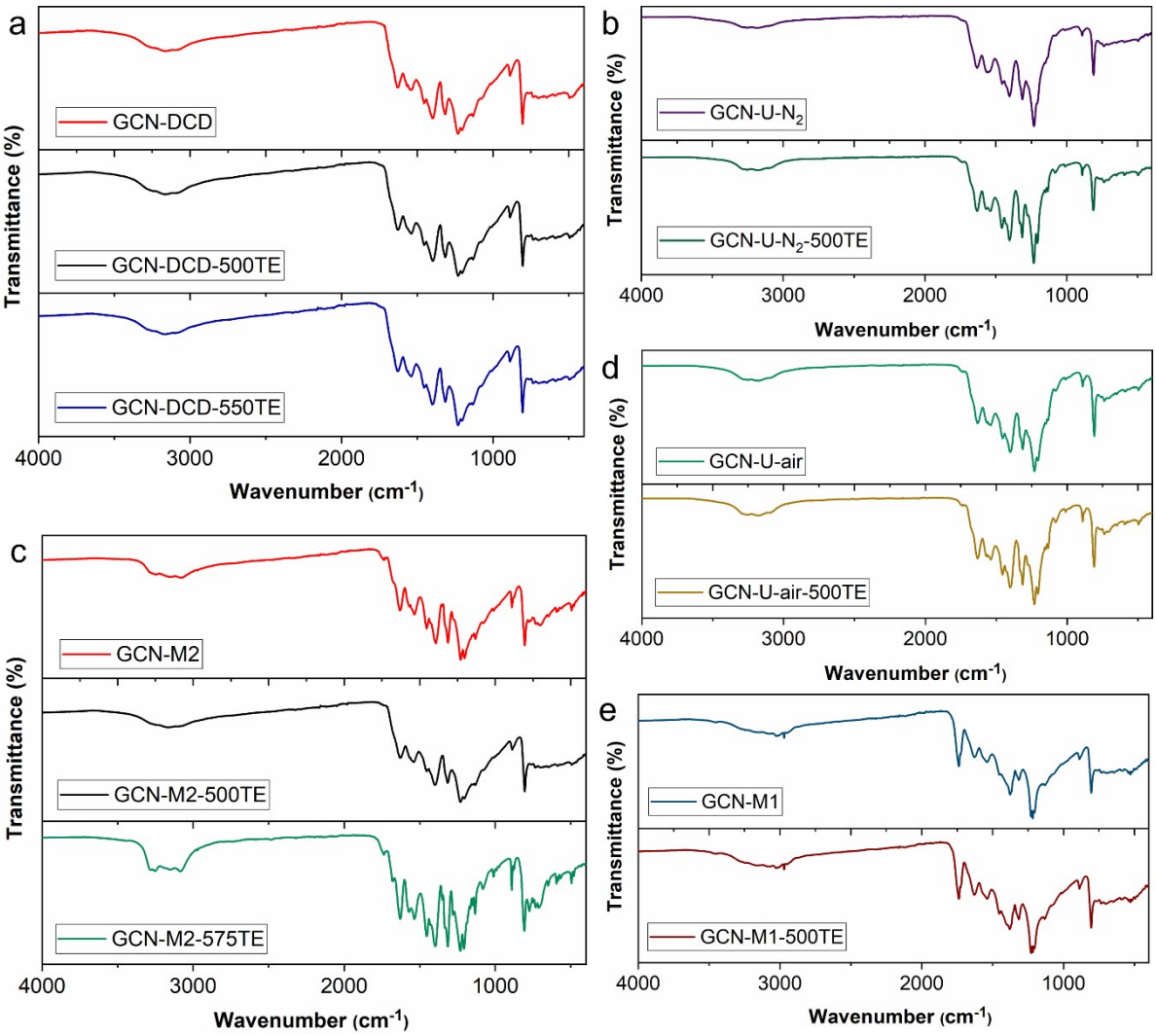

Figure S5 | IR spectra of GCN-X and GCN-X-TE samples. **a.** GCN-DCD, **b.** GCN-U-N_2, **c.** GCN-M2, **d.** GCN-U-air, and **e.** GCN-M1.

1.3. DRS

The comparison of absorption spectra of GCN-X and GCN-X-TE samples showed a red shift in absorption tail for GCN-X samples. This suggests that the GCN-X samples possess a higher degree of polymerization and therefore lower band gaps.[1]

Furthermore, GCN-X-TE possess a lower degree of polymerization and exhibit a blue shift (Figure S6,7). This is in line with the band gaps of GCN-X-TE samples calculated using Tauc plots where band gaps increase with the increase in exfoliation temperatures (Figure S8,9, Table S1). This behavior is observed due to shift of conduction band and valence band in opposite directions and quantum confinement effect, which is similarly observed in previously reported studies.[2,3]

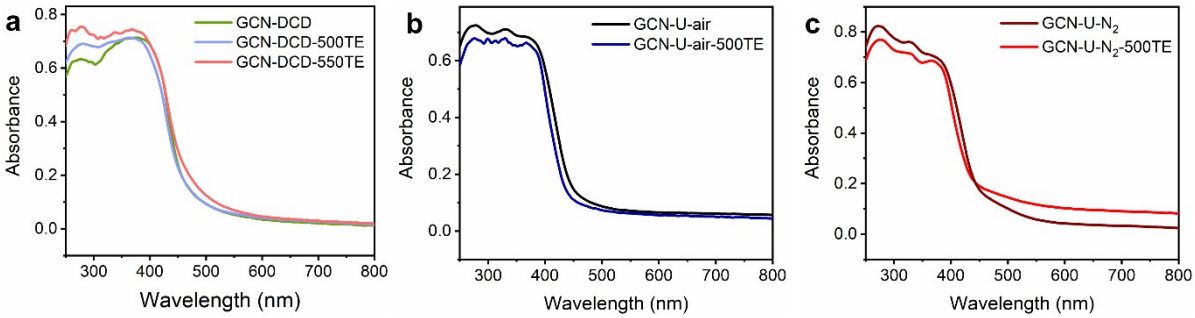

Figure S6 | DRS spectra of GCN-X and GCN-X-TE samples. **a.** GCN-DCD **b.** GCN-U-air, and **c.** GCN-U-N_2.

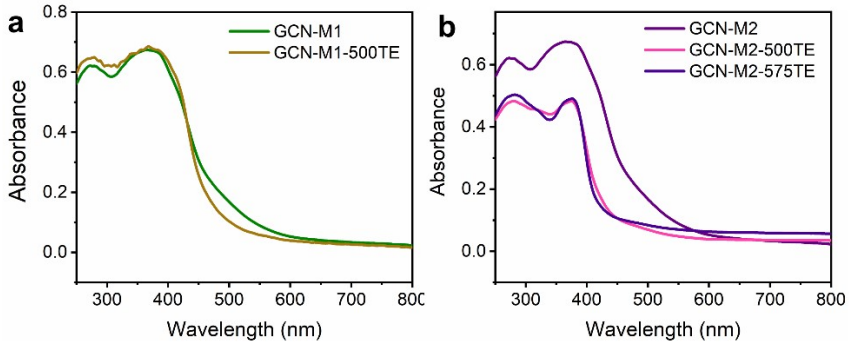

Figure S7 | DRS spectra of GCN-X and GCN-X-TE samples. **a.** GCN-M1, and **b.** GCN-M2.

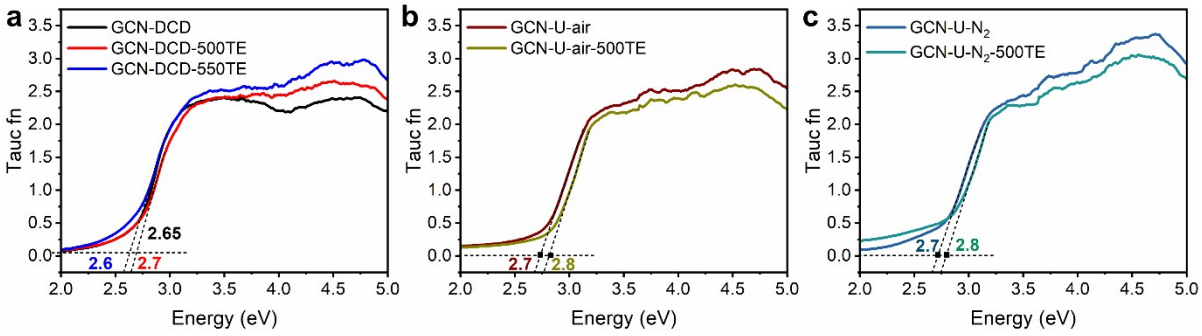

Figure S8 | Tauc plots. **a.** GCN-DCD **b.** GCN-U-air, and **c.** GCN-U-N_2.

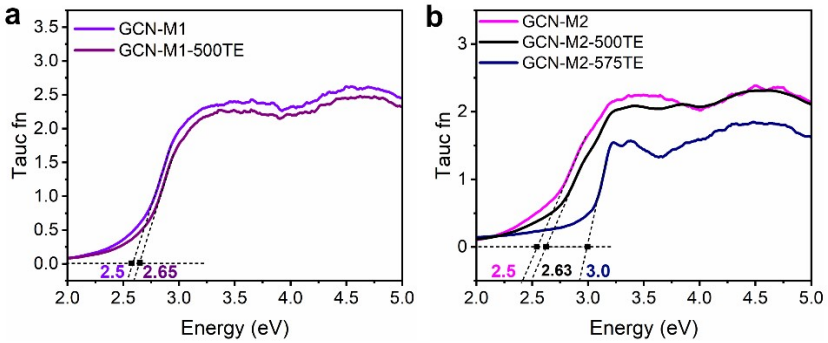

Figure S9 | Tauc plots. **a.** GCN-M1, and **b.** GCN-M2.

Table S1 | Table lists the band gaps of GCN-X and GCN-X-TE samples calculated using Tauc plots and percentage yields obtained after synthesis.

Samples	Band gaps				Yield
	WTE*	500 TE	550 TE	575 TE	WTE** (%)
GCN-DCD	2.65	2.7	2.6	-	30.0
GCN-U-air	2.7	2.8	-	-	2.70
GCN-U-N_2	2.7	2.8	-	-	0.75
GCN-M1	2.5	2.65	-	-	30.0
GCN-M2	2.5	2.63	-	2.9	31.2

TE: Thermal exfoliation; *WTE: Without thermal exfoliation. Yield WTE** is the mass% of the GCN produced relative to the mass of the starting precursor.

2. Charge recombination analysis by photoluminescence spectroscopy (PL)

Photoluminescence spectroscopy (PL) was done to investigate the effect of different synthesis procedures, precursors, and post-annealing temperatures on the PL quenching of GCN (see experimental section for more details). The degree of polymerization as well as the interplanar van der Waals interactions greatly impact the PL quenching of GCN-X.[4] The PL emission intensity is directly related to the extent of charge recombination in different carbon nitride materials. Overall, the GCN-X and GCN-X-TE samples show two emission maxima at 440 nm and 480 nm assigned to the π-π* and n-π* transitions.[5,6] Figure S10a shows that the PL emission intensity quenches in the following order: GCN-U-N_2 > GCN-M1 > GCN-U-air > GCN-DCD, with GCN-U-N_2 exhibiting least charge recombination. In conjunction with the XRD data (section 3.1, Figure 2a), the higher degree of interlayer interaction reduces the charge separation. A similar trend can be observed from time-resolved PL profiles in Figure S11 as catalytically most active 1Pt/GCN-U-N_2 and 1Pt/GCN-M1 samples also exhibit the smallest lifetimes (Table S2) suggesting effective extraction of charge carriers from the GCN backbone.

Table S2 | Excited state lifetimes of the GCN-X samples derived by fitting the PL decay curves from Figure S11.

Sample	Lifetime (ns)
GCN-M1	7.12 ± 0.14
GCN-U-N_2	9.72 ± 0.27
GCN-DCD	10.52 ± 0.15
GCN-U-air	10.56 ± 0.11
GCN-M2	10.62 ± 0.09

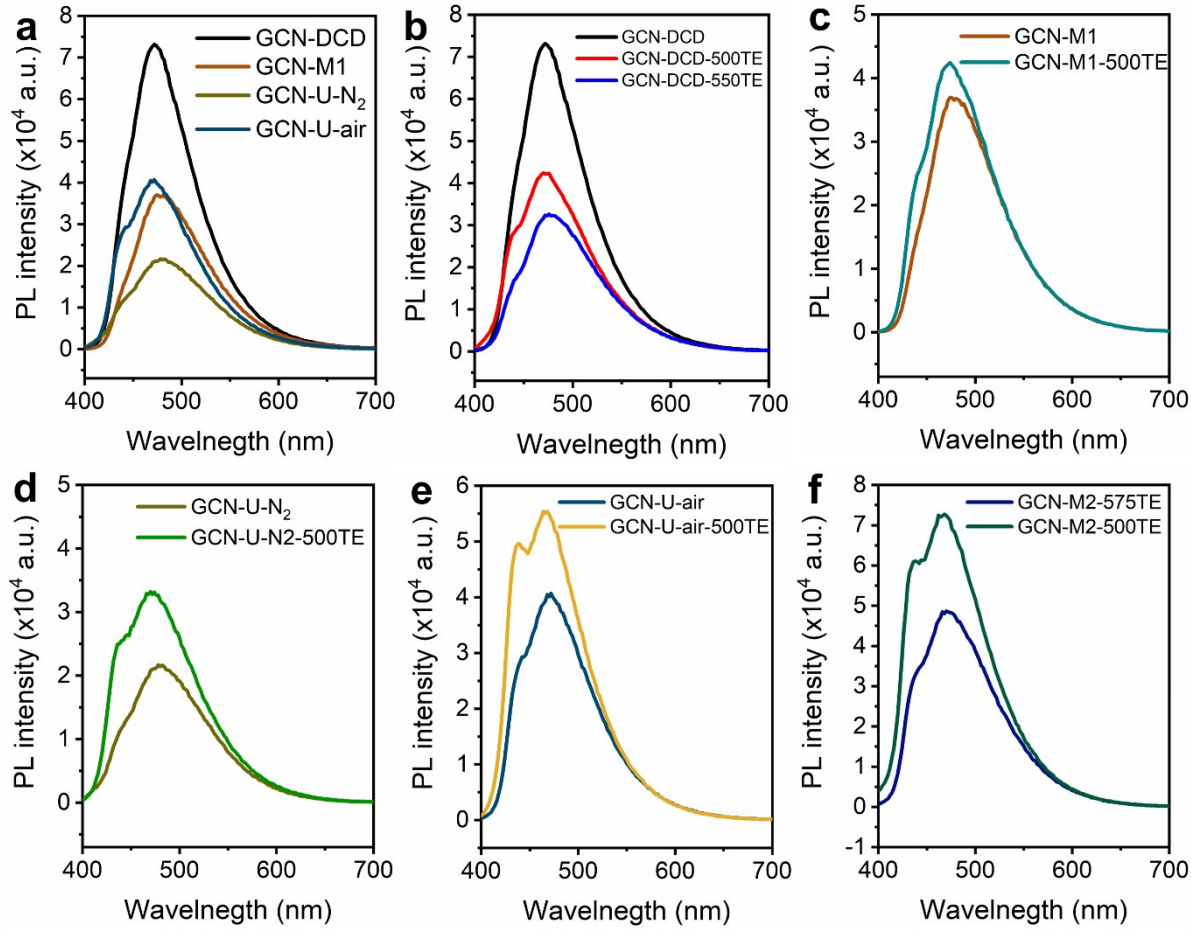

Figure S10 | PL spectra of GCN-X and GCN-X-TE samples. **a.** Comparison of GCN-X samples, **b.** GCN-DCD, **c.** GCN-M1, **d.** GCN-U-N_2, **e.** GCN-U-air, **f.** GCN-M2.

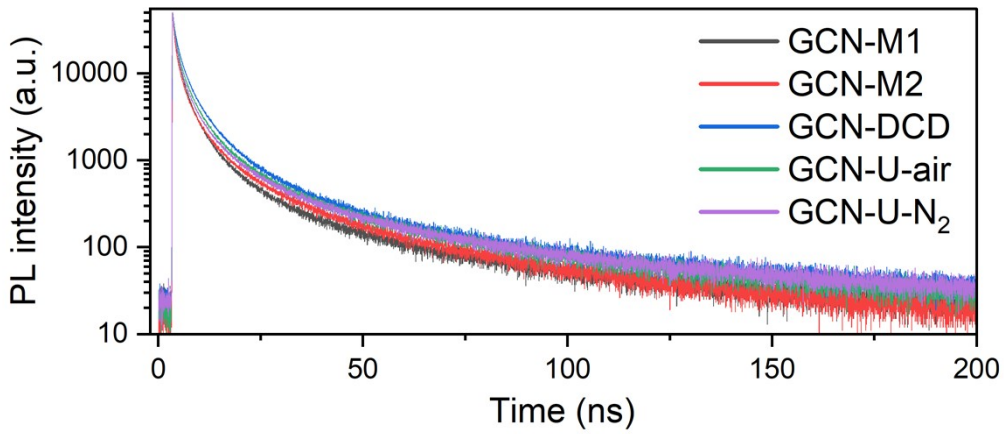

Figure S11 | Time-resolved PL spectra of the GCN-X samples acquired 377 nm laser excitation.

3. BET

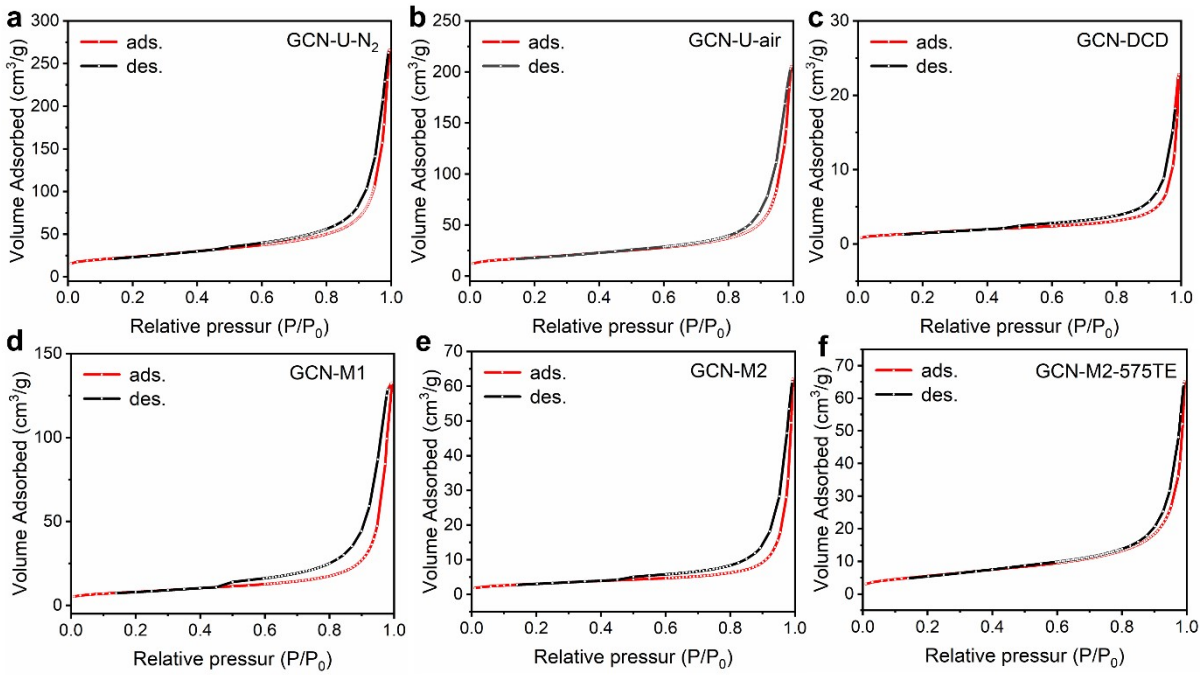

Figure S12 | N_2 adsorption-desorption isotherms recorded for the **a.** GCN-U-N_2, **b.** GCN-U-air, **c.** GCN-DCD, **d.** GCN-M1, **e.** GCN-M2, **f.** GCN-M2-575TE. Details on the values of the BET surface area are presented in Table 2.

4. HER experiments in batch

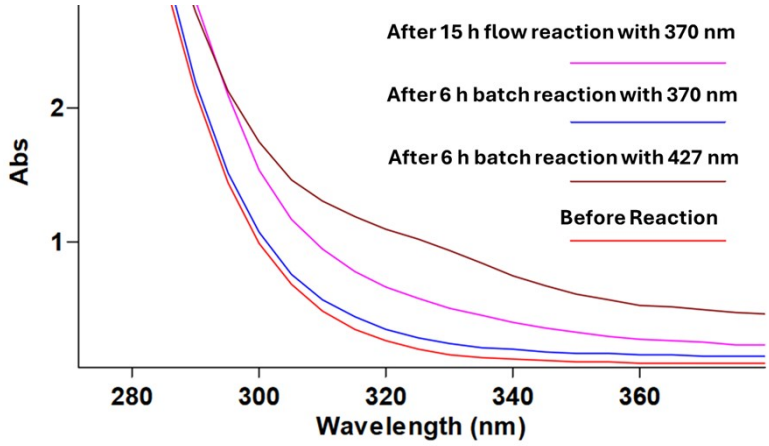

Figure S13 | UV-vis absorbance of the HER reaction solution before reaction compared to the absorbance of the supernatant separated from the catalyst by centrifugation.

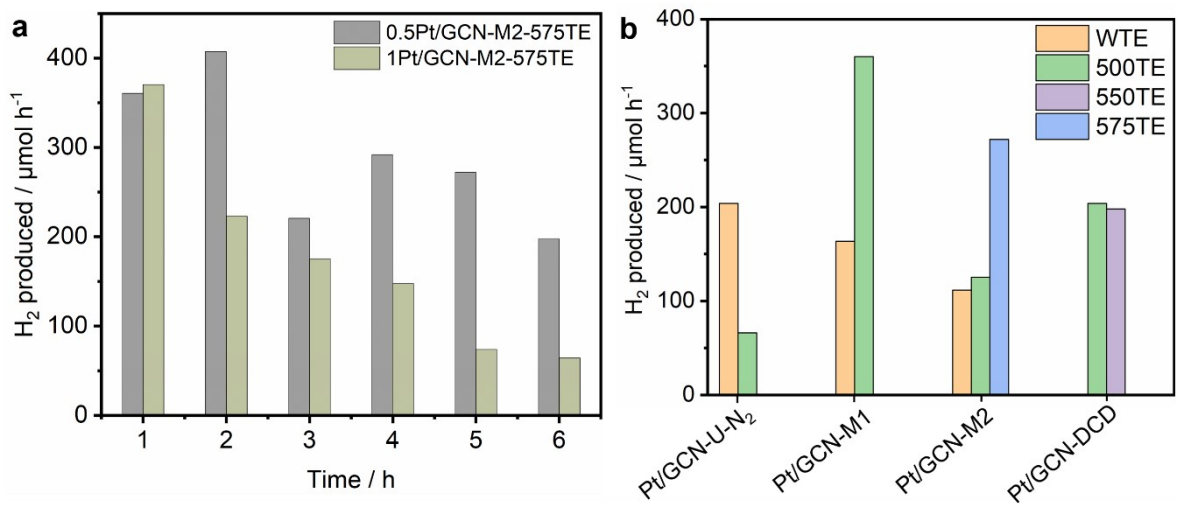

Figure S14 | Photocatalytic HER performance. **a.** Effect of different Pt loadings, **b.** Comparison of HER activities of non-thermally treated GCN-X and thermally treated GCN-X-TE samples at different temperatures after 5 h at 0.5 wt.% Pt loading. The experiments were conducted using 370 nm lamp illuminating photocatalyst suspension having 0.5 and 1 wt.% Pt, prepared in 9:1 vol.% MeOH:H_2O solvent mixture.

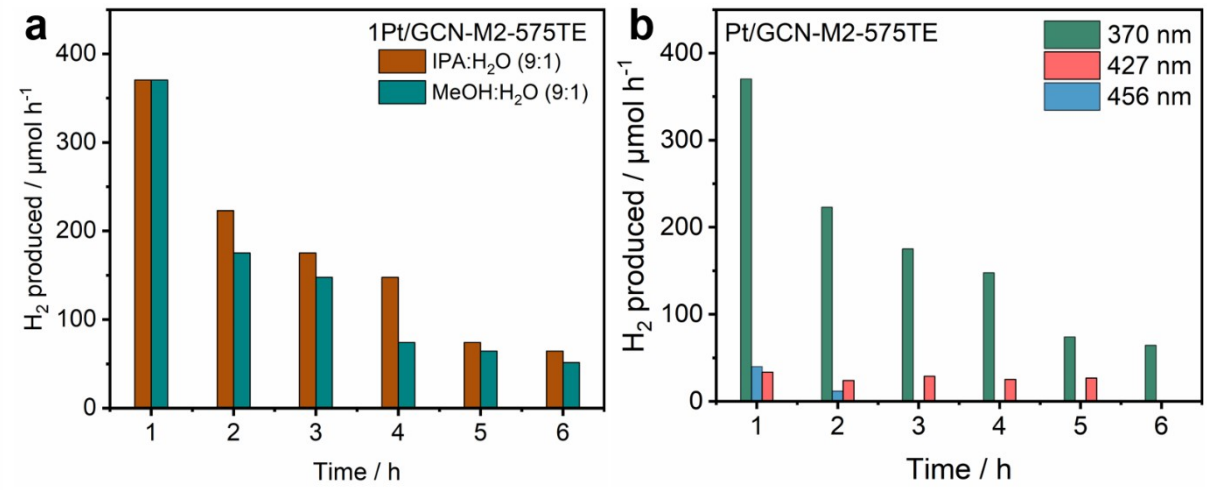

Figure S15 | Comparison of photocatalytic HER performance of Pt/GCN-M2-575TE with **a.** different sacrificial agents, **b.** UV (370 nm) and visible light illumination (427 nm and 456 nm)**.** The experiments were conducted by illuminating photocatalyst suspension having 1 wt.% Pt, prepared in 9:1 vol.% MeOH:H_2O solvent mixture.

5. HER experiments in flow

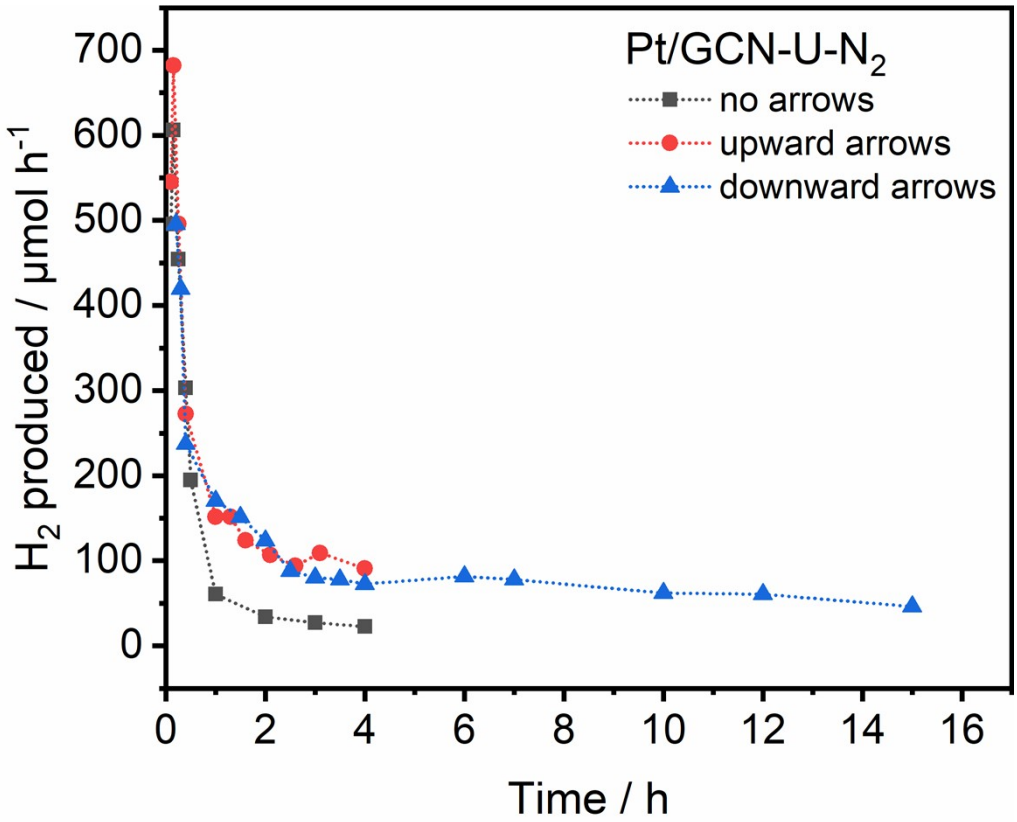

Figure S16 | Comparison of photocatalytic HER performance versus time of Pt/GCN-U-N_2 in three different photo flow reactor configurations. The experiments were conducted by illuminating photocatalyst slurry (2 mg/ ml) having 0.5 wt.% Pt, prepared in 9:1 vol.% MeOH:H_2O solvent mixture and flowing at 20 ml/min. The reactors were illuminated by 370 nm light source.

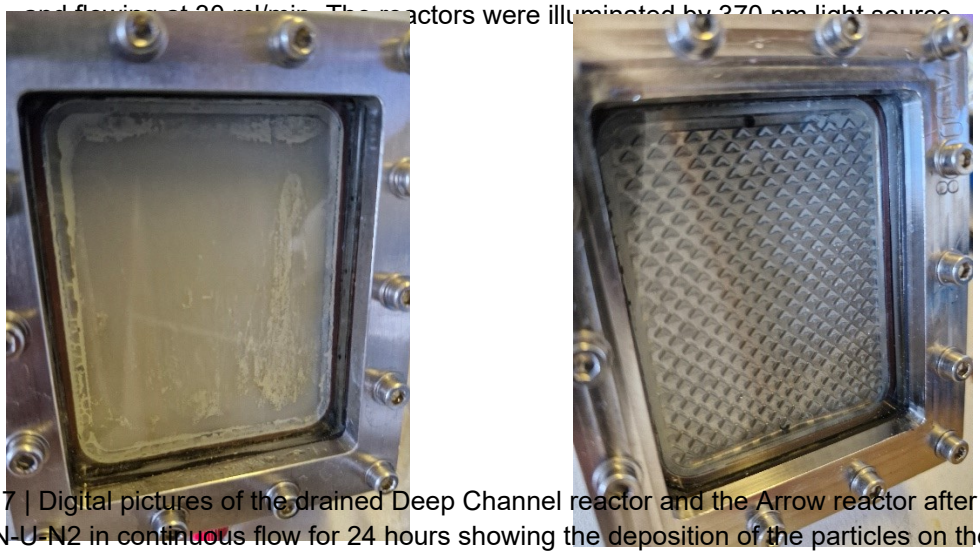

Figure S17 | Digital pictures of the drained Deep Channel reactor and the Arrow reactor after HER with Pt/GCN-U-N2 in continuous flow for 24 hours showing the deposition of the particles on the Deep Channel reactor.

6. White light source intensity

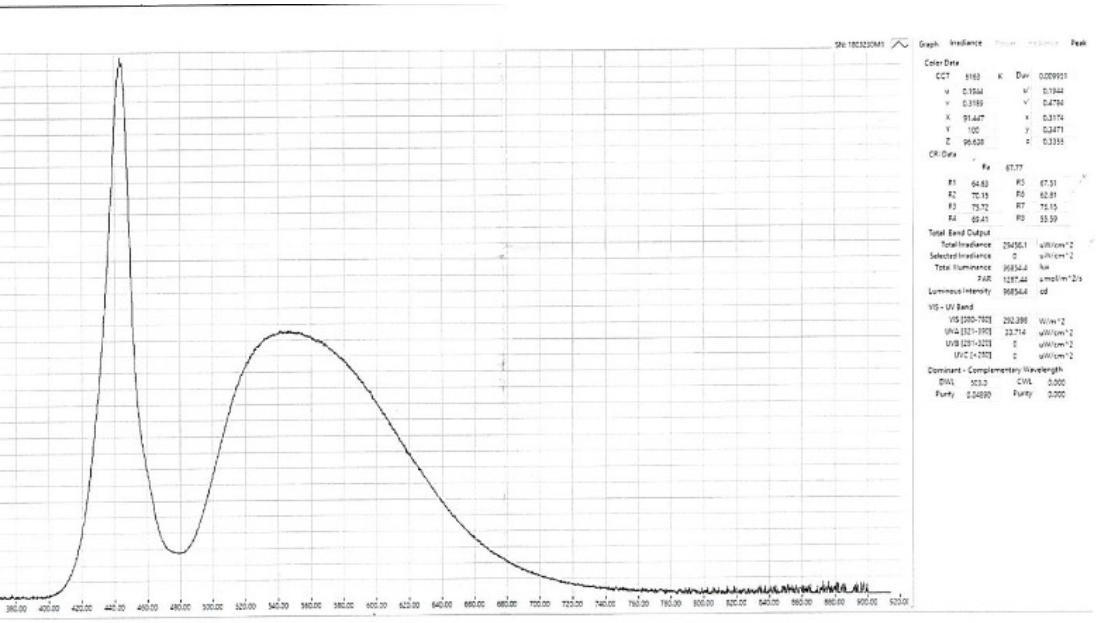

Figure S18 | intensity of the used white light source in batch experiment in Figure 2d.

References

1 J. Bian, J. Li, S. Kalytchuk, Y. Wang, Q. Li, T. C. Lau, T. A. Niehaus, A. L. Rogach and R.-Q. Zhang, *ChemPhysChem*, 2015, **16**, 954–959.

2 N. A. Mohamed, J. Safaei, A. F. Ismail, M. F. A. M. Jailani, M. N. Khalid, M. F. M. Noh, A. Aadenan, S. N. S. Nasir, J. S. Sagu and M. A. M. Teridi, *Appl. Surf. Sci.*, 2019, **489**, 92–100.

3 Q. Gu, Z. Gao, H. Zhao, Z. Lou, Y. Liao and C. Xue, *RSC Adv.*, 2015, **5**, 49317–49325.

4 Y. Zhang, Q. Pan, G. Chai, M. Liang, G. Dong, Q. Zhang and J. Qiu, *Sci. Rep.*, 2013, **3**, 1943.

5 D. Das, D. Banerjee, D. Pahari, U. K. Ghorai, S. Sarkar, N. S. Das and K. K. Chattopadhyay, *J. Lumin.*, 2017, **185**, 155–165.

6 S. Batool, J. S. Schubert, P. Ayala, H. Saito, M. J. Sampaio, E. S. D. Silva, C. G. Silva, J. L. Faria, D. Eder and A. Cherevan, *Sustain. Energy Fuels*, 2024, **8**, 1225–1235.